

Lossless Data Hiding based on Histogram Modification

T. Vijayan, Abinethri and B. Kalaiselvi

Abstract--- *In this, we present a reversible data hiding scheme based on histogram modification. We exploit a binary tree structure to solve the problem of communicating pairs of peak points. Distribution of pixel differences is used to achieve large hiding capacity while keeping the distortion low. We also adopt a histogram shifting technique to prevent overflow and underflow. Performance comparisons with other existing schemes are provided to demonstrate the superiority of the proposed scheme. In this letter, we present a reversible data hiding scheme based on histogram modification. We exploit a binary tree structure to solve the problem of communicating pairs of peak points. Distribution of pixel differences is used to achieve large hiding capacity while keeping the distortion low. We also adopt a histogram shifting technique to prevent overflow and underflow.*

Keywords--- *Underflow, Histogram Modification, Lossless Data.*

I. INTRODUCTION

Lossless data hiding is the technique that allows embedding (hide) data inside an image and later the hidden data can be retrieved as required and the exact copy of the original image is found. One of the most important requirements of reversible data hiding is that the distortions to the original signal should be such that artifacts are not visible. Because these medical, astronomical, and military images due to legal distortions create problems in some fields such as reasons. Another requirement is to have higher embedding capacity.

Data hiding is a term encompassing a wide range of applications for embedding messages in content. Inevitably, hiding information destroys the host image even though the distortion introduced by hiding is imperceptible to the human visual system. There are, however, some sensitive images for which any embedding distortion of the image is intolerable, such as military images, medical images, or artwork preservation. For medical images, even slight changes are unacceptable because of the potential risk of physician misinterpreting the image.

Consequently, reversible data hiding techniques are designed to solve the problem of lossless embedding of large messages in digital images so that after the embedded message is extracted, the image can be completely restored to its original state before embedding occurred.

Existing methods are LSB and Difference expansion methods. A lossless generalized LSB embedding scheme (G-LSB) presented by Celik, uses a variant of an arithmetic compression algorithm to encode a message and hide the resulting interval number in the host image. Tian devised a high-capacity reversible data hiding technique called difference expansion (DE), in which the message is embedded based on the 1-D Haar wavelet transform. The

T. Vijayan, Assistant Professor, School of Electrical Engineering, Department of Electronics and Instrumentation Engineering, BIST, BIHER, Bharath Institute of Higher Education & Research, Selaiyur, Chennai. E-mail: tvij16@gmail.com

Abinethri, Assistant Professor, School of Electrical Engineering, Department of Electronics and Instrumentation Engineering, BIST, BIHER, Bharath Institute of Higher Education & Research, Selaiyur, Chennai.

B. Kalaiselvi, Assistant Professor, School of Electrical Engineering, Department of Electronics and Instrumentation Engineering, BIST, BIHER, Bharath Institute of Higher Education & Research, Selaiyur, Chennai.

resulting high-pass bands are the difference between adjacent pixel values. Tian's technique has been extended recently. Another novel histogram-based reversible data hiding technique was presented by Ni, in which the message is embedded into the histogram bin. They used peak and zero points to achieve low distortion, but with low capacity. Histogram modification techniques have been extended recently. However, those techniques all suffer from the unresolved issue represented by the need to communicate pairs of peak and zero points to recipients.

In this, we extend the histogram modification technique using pixel differences to increase hiding the host image. Tian devised a high-capacity reversible data hiding technique called difference expansion (DE), in which the message is embedded based on the 1-D Haar wavelet transform. The resulting high-pass bands are the differences between adjacent pixel values. Tian's technique capacity. We use a binary tree structure to eliminate the requirement to communicate pairs of peak and zero points to the recipient. We also adopt a histogram shifting technique to prevent overflow and underflow.

II. PROPOSED SCHEME

A lossless data hiding scheme based on histogram modification using pairs of peak and zero points. Let P be the value of peak point and Z be the value of zero point.

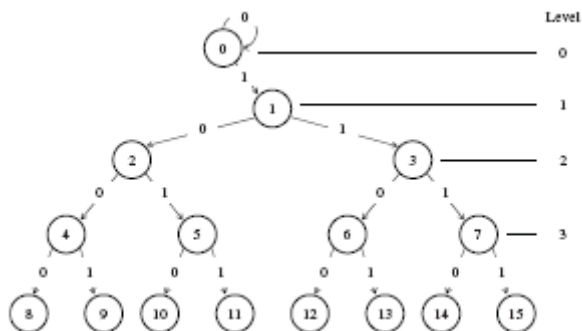
The range of the histogram, $P + 1, Z - 1$, is shifted to the right-hand side by 1. Once a pixel with value P is encountered, if the message bit is "1," the pixel value is increased by 1. Otherwise, no modification is needed. Data extraction is actually the reverse of the data hiding process. Note that the number of message bits that can be embedded into an image equals the number of pixels associated with the peak point. However, the histogram modification technique does not work well when an image has an equal histogram.

While multiple pairs of peak and minimum points can be used for embedding, the pure payload is still a little low. Moreover, the histogram modification technique carries with it an unsolved issue in that multiple pairs of peak and minimum points must be transmitted to the recipient via a side channel to ensure successful restoration. Thus, we present an efficient extension of the histogram modification technique by considering the differences between adjacent pixels instead of simple pixel value. Since image neighbor pixels are strongly correlated, the distribution of pixel difference has a prominent maximum, that is, the difference is expected to be very close to zero. We can find that the differences have almost a zero-mean and Laplacian-like distribution. Distributions of other images also follow this model. Laplacian data can be applied to data hiding schemes to improve their embedding ability. This observation leads us toward designs in which the embedding is done in pixel differences. We also use a tree structure to solve the issue of communicating multiple pairs of peak points to recipients. Having explained our background logic, we now outline the principle of the proposed reversible data hiding algorithm.

III. BINARY TREE STRUCTURE

Fig. 1 shows an auxiliary binary tree for solving the issue of communication of multiple peak points. Each element denotes a peak point. Let us assume that the number of peak points used to embed messages is 2^L , where L is the level of the binary tree. Once a pixel difference d_i that satisfies $d_i < 2^L$ is encountered, if the message bit to be embedded is "0," the left child of the node d_i is visited; otherwise, the right child of the node d_i is visited. Higher

payload require the use of higher tree levels, thus quickly increasing the distortion in the image beyond acceptable levels. However, all the recipient needs to share with the sender is the tree level L, because we propose an auxiliary binary tree that predetermines multiple peak points used to embed messages. A detailed embedding algorithm with the auxiliary binary tree is given later in this method.



Fig(1) Binarytree Structure

IV. HISTOGRAM:-

Color Histogram:-

A color histogram is a representation of the distribution of colors in an image. For digital images, it is basically the number of pixels that have colors in each of a fixed list of color ranges that span the image's color space, the set of all possible colors. histogram can be formed by first normalizing counting histogram of an image is produced first by discretization of the colors in the image into a number of bins, and chromaticity he number of image pixels in each bin.

Grayscale Histogram:-

Here we use 8bit grayscale image the histogram of an image normally refers to a histogram of the pixel intensity values. This histogram is a graph showing the number of pixels in an image at each different intensity value found in that image. For an 8-bit grayscale image there are 256 different possible intensities, and so the histogram will graphically display 256 numbers showing the distribution of pixels amongst those grayscale values.

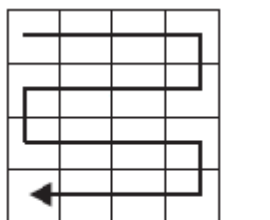
Histogram modification:-

(a) Histogram shifting

Firstly introduced a reversible data hiding technique based on histogram shifting (some times referred to as histogram modification) that we shall describe briefly in this section. Let P_{max} be a pixel value that corresponds to the peak point of image histogram, and all the pixels whose values are larger (or smaller) than P_{max} are increased (or decreased) by 1. The whole image has no pixel whose value is equal to $P_{max}+1$ (or $P_{max}-1$) after histogram shifting. Therefore, P_{max} can be selected to embed data. When embedding a bit 1, P_{max} is modified to $P_{max}+1$ (or $P_{max}-1$), otherwise P_{max} remains intact. Obviously, the amount of message that can be embedded into an image equals to the number of pixels which are associated with the peak point. Because few images contain a large number of pixels with equal gray values.

(b)Extended histogram modification

In 2008, in order to achieve high embedding capacity scheme and presented a new scheme based on histogram modification. By calculating the differences between adjacent pixels instead of simple pixel values, they extended histogram modification scheme. Since the pixel grayscale values in a local are often highly correlated and spatial redundancy, the distribution of pixel difference has a prominent maximum .Hence, their scheme can offer higher embedding capacity and keep lower distortion . However, once the differences between adjacent pixels in a certain sequential order are utilized to embed data, the distribution of pixel difference does not maintain a prominent maximum. This means that the performance of their scheme will drastically decline after the initial period embedding is applied .In order to obtain all-directional adjacent pixel differences of a cover image, various scan paths could be defined. Nine basic scan paths are defined .For simplicity, the basic scan paths are shown for 4×4regions, as shown in Fig.2.a. Let I be a grayscale image with H-row×W-column pixels, in which each pixel take up 8 bits. After one scan path is assigned , we can obtain a series of pixel values p1, p2, p3, ..., pk along the pre-assigned scan path, we have k = H×W.



(a)

Fig(4)scanpath

(c)Adjacent pixel difference

As mentioned above, for a cover image, we can obtain series of pixel values p1, p2, p3, ..., pk along a preassigned scan path. Hence, we can compute k-1 adjacent pixel differences, and the sequence of adjacent pixel differences is defined as <d1, d2, d3, ..., dk-1>, and di is given

$$d_i = p_{i+1} - p_i .$$

For simplicity, in this, the terms “adjacent pixel difference” and “pixel difference” are interchangeable. The histogram of the pixel differences of image Lena with size 512×512×8 , where the pre-assigned scan path are path s2. It is easy to see the difference histogram contains a larger number of points with equal values than image histogram

(d)Prevent Overflow and Underflow:-

Modification of a pixel may not be allowed if the pixel is saturated (0 or 255). To prevent overflow and underflow, we adopt a histogram shifting technique that narrows the histogram from both sides . Let us assume that the number of peak points used to embed messages is 2^L , where L is the level of the proposed binary tree structure. Thus, we shift the histogram from both sides by 2^L units to prevent overflow and underflow since the pixel xi that satisfies $d_i \geq 2^L$, will shift by 2^L units after embedding takes place. After narrowing the histogram to the range 2^L , to $255 - 2^L$, we must record the histogram shifting information as overhead book keeping information. For

this purpose, we create a one bitmap as the location map, which is equal in size to the host image. For a pixel having grayscale value in the range 2^L , $255 - 2^L$, we assign a value 0 in the location map; otherwise, we assign a value 1. The location map is losslessly compressed by the run-length coding algorithm, which will yield a large increase in compression ability since pixels out of the range 2^L to $255 - 2^L$ are few and are almost always contiguous. The overhead information will be embedded into the host image together with the embedded message. Note that the maximum modification to a pixel is limited to 2^L , according to the proposed tree structure. As a result, shifting the histogram from both sides by 2^L units enables us to avoid the occurrence of overflow and underflow.

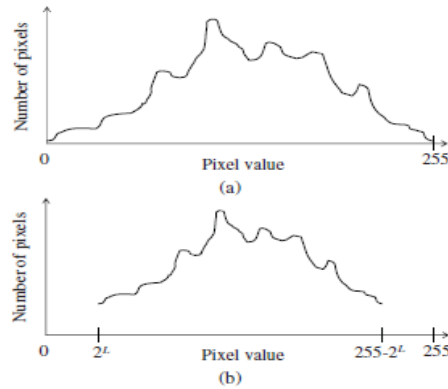


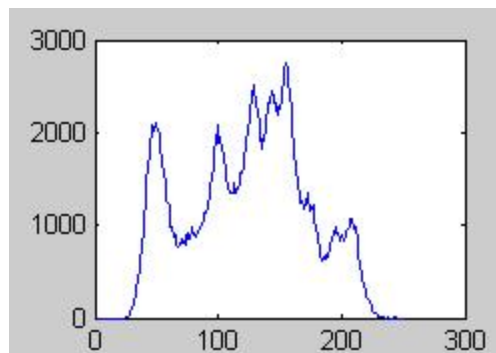
Fig5 Histogram shifting. (a) Original histogram. (b) Histogram shifting

Example:-

4a) Lena image



4b) histogram modification graph



V. EMBEDDING PROCESS

For an N-pixel 8-bit grayscale host image H with a pixel value x_i , where x_i denotes the grayscale value of the i th pixel, $0 \leq i \leq N - 1$, $x_i \in \mathbb{Z}$, $x_i \in (0, 255)$.

- 1) Determine the level L of the binary tree.
- 2) Shift the histogram from both sides by 2^L units. Note that the histogram shifting information is recorded as overhead bookkeeping information that will be embedded into the image itself with payload.
- 3) Scan the image H in an inverse s-order. Calculate the pixel difference d_i between pixels x_{i-1} and x_i .
- 4) Scan the whole image in the same inverse s-order. If $d_i \geq 2^L$, shift x_i by 2^L units

$$y_i = \begin{cases} x_i, & \text{if } i = 0 \\ x_i + 2^L, & \text{if } d_i \geq 2^L \text{ and } x_i \geq x_{i-1} \\ x_i - 2^L, & \text{if } d_i \geq 2^L \text{ and } x_i < x_{i-1} \end{cases}$$

where y_i is the watermarked value of pixel i .

- 5) If $d_i < 2^L$, modify x_i according to the message bit

$$y_i = \begin{cases} x_i + (d_i + b), & \text{if } x_i \geq x_{i-1} \\ x_i - (d_i + b), & \text{if } x_i < x_{i-1} \end{cases}$$

where b is a message bit to be embedded and $b \in \{0, 1\}$. Note that the overhead information is included in the image itself with payload. Thus, the real capacity Cap that is referred to as pure payload is $Cap = Np - |O|$, where Np is the number of pixels that are associated with peak points and $|O|$ is the length of the overhead information.

VI. 6. EXTRACTION PROCESS:-

This process extracts both overhead information and payload from the watermarked image and losslessly recovers the host image. Let L be the level of the proposed binary tree. For an N-pixel 8-bit watermarked image W with a pixel value y_i , where y_i denotes the grayscale value of the i th pixel, $0 \leq i \leq N - 1$, $y_i \in \mathbb{Z}$, $y_i \in (0, 255)$.

- 1) Scan the watermarked image W in an inverse s order
- 2) If $|y_i - x_{i-1}| < 2^{L+1}$, extract message bit b

$$b = \begin{cases} 0, & \text{if } |y_i - x_{i-1}| \text{ is even} \\ 1, & \text{if } |y_i - x_{i-1}| \text{ is odd} \end{cases}$$

where x_{i-1} denotes the restored value of y_{i-1}

- 3) Restore the original value of host pixel x_i by

$$x_i = \begin{cases} y_i + \left\lceil \frac{|y_i - x_{i-1}|}{2} \right\rceil & \text{if } |y_i - x_{i-1}| < 2^{L+1} \text{ and } y_i < x_{i-1} \\ y_i - \left\lceil \frac{|y_i - x_{i-1}|}{2} \right\rceil & \text{if } |y_i - x_{i-1}| < 2^{L+1} \text{ and } y_i > x_{i-1} \\ y_i + 2^L, & \text{if } |y_i - x_{i-1}| \geq 2^{L+1} \text{ and } y_i < x_{i-1} \\ y_i - 2^L, & \text{if } |y_i - x_{i-1}| \geq 2^{L+1} \text{ and } y_i > x_{i-1} \\ y_i, & \text{otherwise.} \end{cases}$$

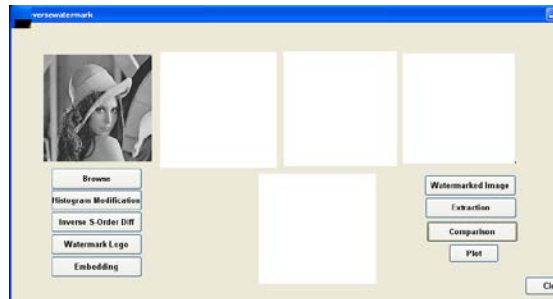
- 4) Repeat Step 2 until the embedded message is completely extracted.

5) Extract the overhead information from the extracted message. If a value 1 is assigned in the location x_i , restore x_i to its original state by shifting it by 2^{L_i} units; otherwise, no shifting is required

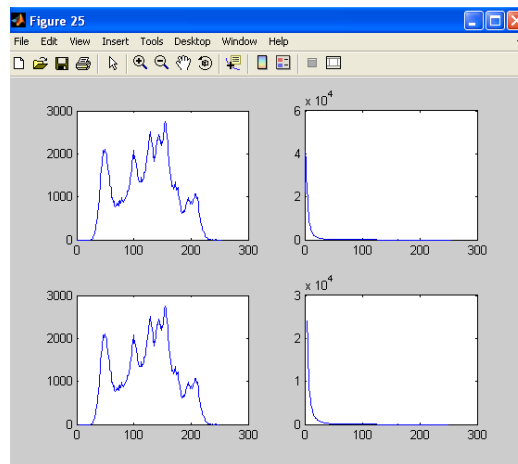
VII. EXPERIMENTAL RESULTS:-

To obtain a better understanding of how different Lena image affect the performance of the proposed reversible data hiding scheme, we present some results in a graphical form. All extraction experiments were performed with Lena grayscale images sized 512x512.

Browse the Image:-



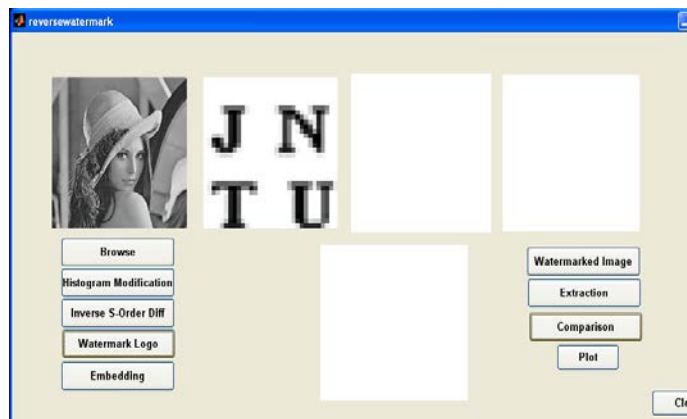
Here we enter binary tree level L=5
 Histogram Graphs:-



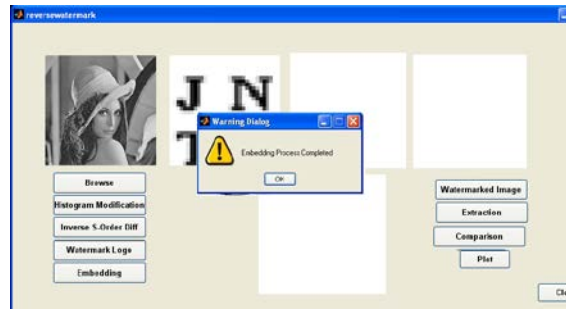
1. Histogram of lean image 2. Distribution of differences 3. Histogram modification of lena image 4. . Distribution of differences

Logo image:-

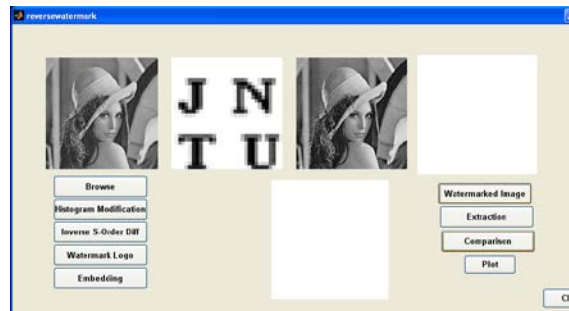
Here we select logo image



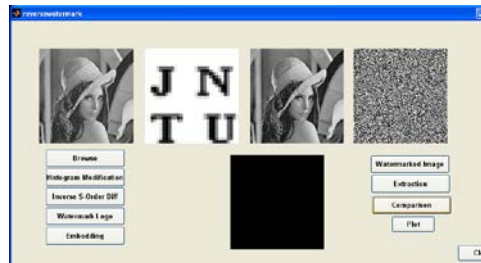
Embedding Process;-



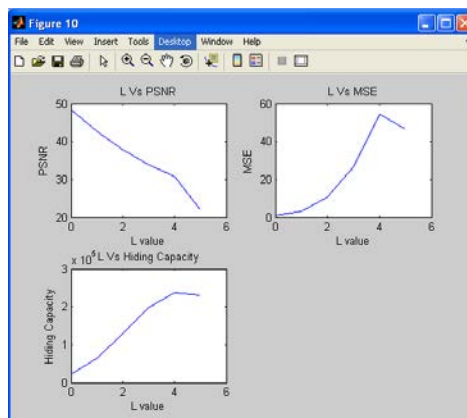
Watermarked Image:-



Comparison:-



In a 4TH figure =input image- Watermarked Image(differences)
 White dots represented differences between input image and Watermarked Image
 In a5th figure =input image –extracted image
 Black represented no difference between input image and extracted image
 Graphs:-



The PSNR block computes the peak signal-to-noise ratio, in decibels, between two images. This ratio is often used as a quality measurement between the original and a extraction image. The higher the PSNR, the better the quality of the extraction image, or reconstructed image.

The Mean Square Error (MSE) and the Peak Signal to Noise Ratio (PSNR) are the two error metrics used to compare image extraction quality. The MSE represents the cumulative squared error between the extraction image and the original image, whereas PSNR represents a measure of the peak error. The lower the value of MSE, the lower the error.

To compute the PSNR, the block first calculates the mean-squared error using the following equation:

$$MSE = \frac{\sum_{M,N} [I_1(m,n) - I_2(m,n)]^2}{M * N}$$

The PSNR is defined as:

$$\begin{aligned} PSNR &= 10 \cdot \log_{10} \left(\frac{MAX_I^2}{MSE} \right) \\ &= 20 \cdot \log_{10} \left(\frac{MAX_I}{\sqrt{MSE}} \right) \end{aligned}$$

Here, MAX_I is the maximum possible pixel value of the image.

VIII. CONCLUSION

In this paper, we have presented an efficient extension of the histogram modification technique by considering the differences between adjacent pixels rather than simple pixel value. One common drawback of virtually all histogram modification techniques is that they must provide a side communication channel for pairs of peak and minimum points. To solve this problem, we introduced a binary tree that predetermines the multiple peak points used to embed messages; thus, the only information the sender and recipient must share is the tree level L. In addition, since neighbor pixels are often highly correlated and have spatial redundancy, the differences have a Laplacian-like distribution. This enables us to achieve large hiding capacity while keeping embedding distortion low.

REFERENCES

- [1] Tamilselvi N., Krishnamoorthy P., Dhamotharan R., Arumugam P., Sagadevan E., Analysis of total phenols, total tannins and screening of phytochemicals in *Indigofera aspalathoides* (Shivanar Vembu) Vahl EX DC, *Journal of Chemical and Pharmaceutical Research*, V-4, I-6, PP:3259-3262, 2012.
- [2] Godlyn Abraham A., Manikandan A., Manikandan E., Jaganathan S.K., Baykal A., Sri Renganathan P., Enhanced opto-magneto properties of Ni x Mg 1-x Fe 2 O 4 (0.0 ≤ x ≤ 1.0) ferrites nano-catalysts, *Journal of Nanoelectronics and Optoelectronics*, V-12, I-12, PP:1326-1333, 2017.
- [3] Barathiraja C., Manikandan A., Uduman Mohideen A.M., Jayasree S., Antony S.A., Magnetically Recyclable Spinel MnxNi1-xFe2 O 4 (x= 0.0–0.5) Nano-photocatalysts: Structural, Morphological and Opto-magnetic Properties, *Journal of Superconductivity and Novel Magnetism*, V-29, I-2, PP:477-486, 2016.
- [4] Kaviyarasu K., Manikandan E., Nuru Z.Y., Maaza M., Investigation on the structural properties of CeO₂ nanofibers via CTAB surfactant, *Materials Letters*, V-160, PP:61-63, 2015.

- [5] Kaviyarasu K., Manikandan E., Maaza M., Synthesis of CdS flower-like hierarchical microspheres as electrode material for electrochemical performance, *Journal of Alloys and Compounds*, V-648, PP:559-563, 2015.
- [6] Sachithanantham P., Sa Nkaran S., Elavenil S., Experimental study on the effect of rise on shallow funicular concrete shells over square ground plan, *International Journal of Applied Engineering Research*, V-10, I-20, PP:41340-41345, 2015.
- [7] Jayalakshmi T., Krishnamoorthy P., Ramesh Kumar G., Sivamani P., Optimization of culture conditions for keratinase production in *Streptomyces* sp. JRS19 for chick feather wastes degradation, *Journal of Chemical and Pharmaceutical Research*, V-3, I-4, PP:498-503, 2011.
- [8] Kumarave A., Rangarajan K., Routing algorithm over semi-regular tessellations, 2013 IEEE Conference on Information and Communication Technologies, ICT 2013, PP:1180-1184, 2013.
- [9] Sonia M.M.L., Anand S., Vinosel V.M., Janifer M.A., Pauline S., Manikandan A., Effect of lattice strain on structure, morphology and magneto-dielectric properties of spinel $\text{NiGd}_x\text{Fe}_{2-x}\text{O}_4$ ferrite nanocrystallites synthesized by sol-gel route, *Journal of Magnetism and Magnetic Materials*, V-466, PP:238-251, 2018.
- [10] Jeyanthi Rebecca L., Susithra G., Sharmila S., Das M.P., Isolation and screening of chitinase producing *Serratia marcescens* from soil, *Journal of Chemical and Pharmaceutical Research*, V-5, I-2, PP:192-195, 2013.
- [11] Banumathi B., Vaseeharan B., Rajasekar P., Prabhu N.M., Ramasamy P., Murugan K., Canale A., Benelli G., Exploitation of chemical, herbal and nanoformulated acaricides to control the cattle tick, *Rhipicephalus (Boophilus) microplus* – A review, *Veterinary Parasitology*, V-244, PP:102-110, 2017.
- [12] Gopinath S., Sundararaj M., Elangovan S., Rathakrishnan E., Mixing characteristics of elliptical and rectangular subsonic jets with swirling co-flow, *International Journal of Turbo and Jet Engines*, V-32, I-1, PP:73-83, 2015.
- [13] Thooyamani K.P., Khanaa V., Udayakumar R., Efficiently measuring denial of service attacks using appropriate metrics, *Middle - East Journal of Scientific Research*, V-20, I-12, PP:2464-2470, 2014.
- [14] Padmapriya G., Manikandan A., Krishnasamy V., Jaganathan S.K., Antony S.A., Enhanced Catalytic Activity and Magnetic Properties of Spinel $\text{MnxZn}_{1-x}\text{Fe}_2\text{O}_4$ ($0.0 \leq x \leq 1.0$) Nano-Photocatalysts by Microwave Irradiation Route, *Journal of Superconductivity and Novel Magnetism*, V-29, I-8, PP:2141-2149, 2016.
- [15] Rajesh E., Sankari L., Malathi L., Krupaa J.R., Naturally occurring products in cancer therapy, *Journal of Pharmacy and Bioallied Sciences*, V-7, PP:S181-S183, 2015.
- [16] Vanangamudi S., Prabhakar S., Thamotharan C., Anbazhagan R., Dual fuel hybrid bike, *Middle - East Journal of Scientific Research*, V-20, I-12, PP:1819-1822, 2014.
- [17] Brindha G., Krishnakumar T., Vijayalatha S., Emerging trends in tele-medicine in rural healthcare, *International Journal of Pharmacy and Technology*, V-7, I-2, PP:8986-8991, 2015.
- [18] Sharmila S., Jeyanthi Rebecca L., Naveen Chandran P., Kowsalya E., Dutta H., Ray S., Kripanand N.R., Extraction of biofuel from seaweed and analyse its engine performance, *International Journal of Pharmacy and Technology*, V-7, I-2, PP:8870-8875, 2015.
- [19] Thooyamani K.P., Khanaa V., Udayakumar R., Using integrated circuits with low power multi bit flip-flops in different approach, *Middle - East Journal of Scientific Research*, V-20, I-12, PP:2586-2593, 2014.
- [20] Thooyamani K.P., Khanaa V., Udayakumar R., Virtual instrumentation based process of agriculture by automation, *Middle - East Journal of Scientific Research*, V-20, I-12, PP:2604-2612, 2014.
- [21] Udayakumar R., Kaliyamurthi K.P., Khanaa, Thooyamani K.P., Data mining a boon: Predictive system for university topper women in academia, *World Applied Sciences Journal*, V-29, I-14, PP:86-90, 2014.
- [22] Anbuselvi S., Jeyanthi Rebecca L., Sathish Kumar M., Senthilvelan T., GC-MS study of phytochemicals in black gram using two different organic manures, *Journal of Chemical and Pharmaceutical Research*, V-4, I-2, PP:1246-1250, 2012.
- [23] Subramanian A.P., Jaganathan S.K., Manikandan A., Pandiaraj K.N., Gomathi N., Supriyanto E., Recent trends in nano-based drug delivery systems for efficient delivery of phytochemicals in chemotherapy, *RSC Advances*, V-6, I-54, PP:48294-48314, 2016.
- [24] Thooyamani K.P., Khanaa V., Udayakumar R., Partial encryption and partial inference control based disclosure in effective cost cloud, *Middle - East Journal of Scientific Research*, V-20, I-12, PP:2456-2459, 2014.

- [25] Lingeswaran K., Prasad Karamcheti S.S., Gopikrishnan M., Ramu G., Preparation and characterization of chemical bath deposited cds thin film for solar cell, Middle - East Journal of Scientific Research, V-20, I-7, PP:812-814, 2014.
- [26] Maruthamani D., Vadivel S., Kumaravel M., Saravanakumar B., Paul B., Dhar S.S., Habibi-Yangjeh A., Manikandan A., Ramadoss G., Fine cutting edge shaped Bi₂O₃rods/reduced graphene oxide (RGO) composite for supercapacitor and visible-light photocatalytic applications, Journal of Colloid and Interface Science, V-498, PP:449-459, 2017.
- [27] Gopalakrishnan K., Sundeeep Aanand J., Udayakumar R., Electrical properties of doped azopolyester, Middle - East Journal of Scientific Research, V-20, I-11, PP:1402-1412, 2014.
- [28] Subhashree A.R., Parameaswari P.J., Shanthi B., Carnagarin R., Parijatham B.O., The reference intervals for the haematological parameters in healthy adult population of Chennai, Southern India, Journal of Clinical and Diagnostic Research, V-6, I-10, PP:1675-1680, 2012.
- [29] Niranjana U., Subramanyam R.B.V., Khanaa V., Developing a Web Recommendation System Based on Closed Sequential Patterns, Communications in Computer and Information Science, V-101, PP:171-179, 2010.
- [30] Slimani Y., Baykal A., Manikandan A., Effect of Cr³⁺ substitution on AC susceptibility of Ba hexaferrite nanoparticles, Journal of Magnetism and Magnetic Materials, V-458, PP:204-212, 2018.
- [31] Premkumar S., Ramu G., Gunasekaran S., Baskar D., Solar industrial process heating associated with thermal energy storage for feed water heating, Middle - East Journal of Scientific Research, V-20, I-11, PP:1686-1688, 2014.
- [32] Kumar S.S., Karrunakaran C.M., Rao M.R.K., Balasubramanian M.P., Inhibitory effects of Indigofera aspalathoides on 20-methylcholanthrene- induced chemical carcinogenesis in rats, Journal of Carcinogenesis, V-10, 2011.
- [33] Beula Devamalar P.M., Thulasi Bai V., Srivatsa S.K., Design and architecture of real time web-centric tele health diabetes diagnosis expert system, International Journal of Medical Engineering and Informatics, V-1, I-3, PP:307-317, 2009.
- [34] Ravichandran A.T., Srinivas J., Karthick R., Manikandan A., Baykal A., Facile combustion synthesis, structural, morphological, optical and antibacterial studies of Bi_{1-x}Al_xFeO₃ (0.0 ≤ x ≤ 0.15) nanoparticles, Ceramics International, V-44, I-11, PP:13247-13252, 2018.
- [35] Thovhogi N., Park E., Manikandan E., Maaaza M., Gurib-Fakim A., Physical properties of CdO nanoparticles synthesized by green chemistry via Hibiscus Sabdariffa flower extract, Journal of Alloys and Compounds, V-655, PP:314-320, 2016.
- [36] Thooyamani K.P., Khanaa V., Udayakumar R., Wide area wireless networks-IETF, Middle - East Journal of Scientific Research, V-20, I-12, PP:2042-2046, 2014.
- [37] Sundar Raj M., Saravanan T., Srinivasan V., Design of silicon-carbide based cascaded multilevel inverter, Middle - East Journal of Scientific Research, V-20, I-12, PP:1785-1791, 2014.
- [38] Achudhan M., Prem Jayakumar M., Mathematical modeling and control of an electrically-heated catalyst, International Journal of Applied Engineering Research, V-9, I-23, PP:23013-, 2014.
- [39] Thooyamani K.P., Khanaa V., Udayakumar R., Application of pattern recognition for farsi license plate recognition, Middle - East Journal of Scientific Research, V-18, I-12, PP:1768-1774, 2013.
- [40] Jebaraj S., Iniyana S., Renewable energy programmes in India, International Journal of Global different solvent extracts of Murraya koenigii, Journal of Chemical and Pharmaceutical Research, V-5, I-2, PP:279-282, 2013.
- [41] Venkatesh Guru, K. (2015). Active Low Energy Outlay Routing Algorithm for Wireless Ad Hoc Network. *International Journal of Communication and Computer Technologies*, 3(1), 6-8.
- [42] Surendheran, A.R., & Prashanth, K. (2015). A Survey of Energy-Efficient Communication Protocol for Wireless Sensor Networks. *International Journal of Communication and Computer Technologies*, 3(2), 50-57.
- [43] Han, D.H., & Nv, Z. (2017). Mining Frequent Patterns in Large Scale Databases Using Adaptive FP-Growth Approach. *Bonfring International Journal of Industrial Engineering and Management Science*, 7(2), 17-20.
- [44] Zahedifard, M., & Attarzadeh, I., Pazhokhzadeh, H., & Malekzadeh, J. (2015). Prediction of students' performance in high school by data mining classification techniques. *International Academic Journal of Science and Engineering*, 2(7), 25-33.
- [45] Poursheikhi, M., & Torkestanib, J.A. (2015). To present the new structure to better manage and control requests in the national information network based SDN architecture. *International Academic Journal of Science and Engineering*, 2(7), 34-50.

- [46] Suganya, M., Bramanayaki, S., Sri Nandhini, S., & Subbulakshmi, P. (2014). Locating Center of Optic Disc in Retinal Images. *International Journal of System Design and Information Processing*, 2(3), 54-58.
- [47] Sivaranjani, S. (2018). Detecting Congestion Patterns in Spatio Temporal Traffic Data Using Frequent Pattern Mining. *Bonfring International Journal of Networking Technologies and Applications*, 5(1), 21-23.
- [48] Smith, J., and Sebastian, J. (2017). Feeder Automation and its Reliability Assessment on the Basis of Cost Analysis for the Distribution of Feeders in Power System Planning. *Bonfring International Journal of Power Systems and Integrated Circuits*, 7(2), 19-26.
- [49] Balagopalan, S., Aravind, T., Sreehari, G.N., Praveesh, V.V., & Padmanabhan, G.G.N. (2014). E-waste Management Schools for the Homeless. *International Scientific Journal on Science Engineering & Technology*, 17(11), 1026-1032.
- [50] Rajendra, M.A., & Puranik Vipin, G. (2014). Airbag Deployment System Based On Pre-crash Information. *International Scientific Journal on Science Engineering & Technology*, 17(10), 975-981